Chemosphere 284 (2021) 131319

Contents lists available at ScienceDirect

Chemosphere

journal homepage: www.elsevier.com/locate/chemosphere

Integrated mathematical model to simulate the performance of a membrane bioreactor

L.M.L.K.B. Lindamulla [a,b], V. Jegatheesan [a,*], K.B.S.N. Jinadasa [b], K.G.N. Nanayakkara [b], M. Z. Othman [a]

[a] School of Engineering, RMIT University, GPO Box 2476, Melbourne, 3001, Australia
[b] Department of Civil Engineering, University of Peradeniya, Peradeniya, 20400, Sri Lanka

ARTICLE INFO

Handling Editor: Derek Muir

Keywords:
AQUASIM
Mathematical modelling
Membrane bioreactor (MBR)
Wastewater treatment

ABSTRACT

Membrane bioreactor technology includes the integration of biological wastewater treatment and physical separation by membrane filtration. When analyzing the system performance, efficiency of biological processes, physical separation and membrane fouling must be taken into consideration. Over the years, mathematical modelling of wastewater treatment has evolved and is being used extensively to optimize the performance of treatment systems. A Number of attempts have been made towards the development of mathematical models for membrane bioreactors and most of these models have not considered the effect of soluble microbial products on membrane fouling. Also the effect of periodic membrane cleaning was neglected. In this study, an integrated mathematical model was developed for the membrane bioreactor. A biological model based on activated sludge processes (extended with biopolymer kinetics) and a physical model with cake layer kinetics and membrane fouling have been combined. In order to overcome the drawbacks of previous attempts of modelling, the influence of soluble microbial products and extracellular polymeric substances are considered in the model integration. Further, the physical processes of the sludge removal and membrane cleaning which have strong influence on membrane fouling are considered in the model. "AQUASIM", a computer program for the identification and simulation of aquatic systems, was used for solving the processes. Calibrated and validated model enables the prediction of the system performance and membrane fouling under different operating conditions.

1. Introduction

Wastewater can be defined as the discharge resulting from domestic, industrial, agricultural or commercial usage of fresh or treated water. Depending on the source of discharge, the composition of wastewater will vary. In general, wastewater will contain suspended solids and dissolved organic and inorganic compounds as well as microorganisms. Untreated or under-treated wastewater will contaminate the environment in a number of ways. Pathogens in wastewater will cause diseases. Harmful chemicals and heavy metals in wastewater can cause a variety of problems to the environment as well as the health of the humans and other life forms (Masindi and Muedi, 2018). Therefore the treatment of all kinds of wastewater before releasing them into the environment is important (Michael et al., 2013). Based on the origin of the wastewater and its constituents, treatment options are selected out of available treatment options (Gogate and Pandit, 2004). Treatment technologies can be categorized as biological, chemical and physical. In most cases, effective treatment systems utilize combination of those options (Crini and Lichtfouse, 2019).

Biological wastewater treatment systems are often combined with physical systems for solid/liquid separation. Biological wastewater treatment utilizes bacteria and other microorganisms to degrade contaminants present in wastewater while allowing those microorganisms to grow as well as to generate associated products (Samer, 2015). Sedimentation tanks are used to separate these solids from the treated water. Number of different configurations of biological wastewater treatment systems can be identified including sequencing batch reactor (Jagaba et al., 2021), rotating biological contactors (Waqas and BILAD, 2019), trickling filters (Naz et al., 2015), moving bed bio reactors (Di Biase et al., 2019) and membrane bioreactors (Judd, 2010) which have evolved over the years to suit different treatment requirements.

Membrane bioreactor (MBR) is a wastewater treatment system where a perm-selective membrane has been used, along with a biological treatment, for solid/liquid separation (Judd, 2010). The membrane is

* Corresponding author.
E-mail address: jega.jegatheesan@rmit.edu.au (V. Jegatheesan).

https://doi.org/10.1016/j.chemosphere.2021.131319
Received 7 April 2021; Received in revised form 27 May 2021; Accepted 21 June 2021
Available online 24 June 2021

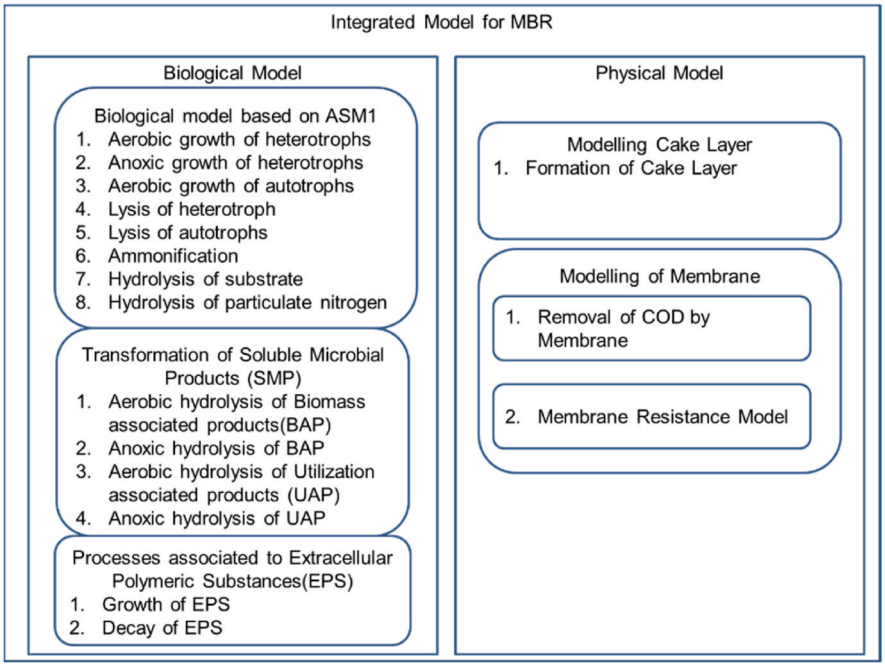

(a)

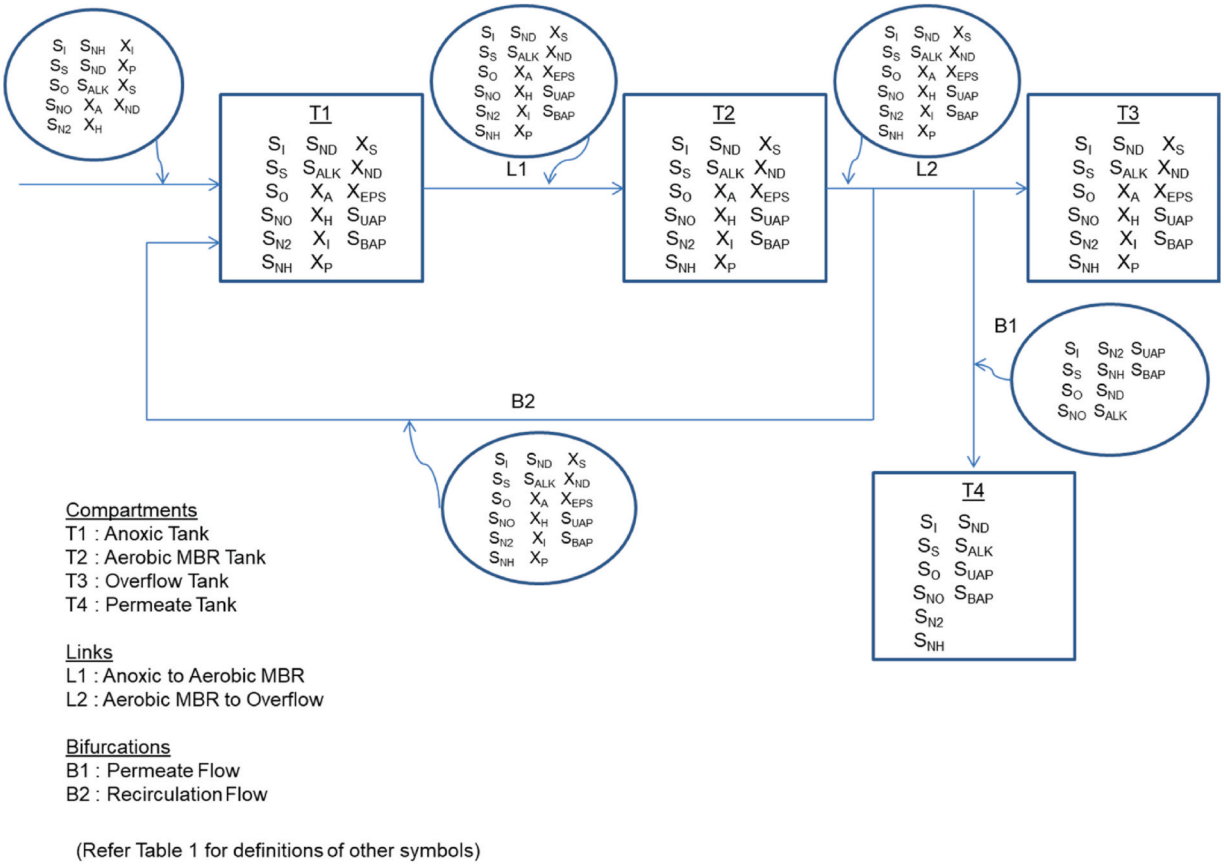

(b)

Fig. 1. (a) Conceptual framework of the integrated model to simulate the performance of a MBR, (b) Compartments and links used in AQUASIM

used as a filtration device to remove solid particles entering the MBR as well as the microbial flocs generated by the biological process. Membrane bioreactors were initially used by Dorr-Oliver for ship-board sewage treatment in late 1960s. There, the conventional activated sludge process was used and it was integrated with an ultrafiltration system (Bemberis, 1971). During late 90's and early 2000, the MBR technology developed rapidly and MBR based treatment systems are implemented throughout the world (El-Fadel et al., 2018).

Membrane bioreactors are classified based on the configuration, type and pore size of the membrane (Abdel-Fatah, 2018). Based on the configuration of the MBRs, they are classified as side-stream or immersed membrane bioreactors (Le-Clech et al., 2005; Morrow et al., 2018). The membranes used in the MBR can be either hollow fiber or flat sheet membranes (Hashisho et al., 2016). Moreover, based on the pore size MBRs can be either ultrafiltration (0.01–0.05 μm) or microfiltration (0.1–0.4 μm) (Abdel-Fatah, 2018).

In general, combining activated sludge units with membrane filtration for biomass retention results in high effluent quality and a compact plant configuration. Despite the benefits of MBR systems, some aspects, particularly membrane permeability and hydraulic performance, need to be better understood in order to maximize their efficiency (Wang et al., 2020). In general, fouling occurs in these systems as a result of the accumulation of substances on the membrane's surface and within its pores (Du et al., 2020). Physical and chemical interactions between the membrane and the mixed liquor have a major effect on the degree and extent of fouling; in particular, the mixed liquor composition determines fouling characteristics (Hamedi et al., 2019). The fouling phenomenon is a contentious problem, and a complete understanding of the physical processes in a MBR plant is still lacking. With this background, mathematical modeling approaches can help in learning more about the factors which affect membrane fouling and MBR efficiency in treating various types of wastewater. Further, a complete model can also be used as an information repository, facilitating collaboration between engineers and scientists. Over the years, a handful of attempts have been made to develop models to simulate the performance of the MBR. In most cases these models have focused on one particular aspect of MBR, namely either the performance of the biological processes occurring in the MBR or the performance of the membrane, the physical system, when determining membrane fouling (Zuthi et al., 2017).

Zarragoitia-González et al. (2008) connected the biological system of activated sludge model (ASM) to a fully-fledged membrane fouling model. ASM1 based model with soluble microbial products (SMP) kinetics was integrated with membrane fouling model by Di Bella et al. (2008). The model did not consider the influence of SMP on the irreversible fouling of the membrane. Mannina et al. (2011) integrated fouling model introduced by Di Bella et al. (2008) with modified ASM1 based model which includes the SMP kinetics. This model also lacks the connection of SMP and irreversible fouling. Janus (2014) developed an integrated mathematical model of MBR where the ASM, membrane fouling and air scouring were considered. Effects of membrane cleaning on membrane fouling and resistance have not been considered in this model.

The main aim of this study is to setup an integrated mathematical model for membrane bioreactor to simulate processes and to aid the design and operation of full scale membrane bioreactors. The processes in MBR are identified under two sections namely biological component and physical component. The components are integrated by identifying the relationships among each other. The biological model was expanded by introducing the kinetics of SMP and extra-cellular polymeric substances (EPS). The fouling of the membrane is proportional to the concentrations of EPS and SMP in the mixed liquor and determines the membrane resistance as well as the trans-membrane pressure (TMP). The model developed in this study overcomes the drawbacks of previous modelling attempts, by integrating the effects of SMP and EPS as well as the impacts of membrane cleaning on membrane fouling and resistance.

2. Modelling of MBR

The MBR model developed in this study consists of two sub models for simulating biological and physical processes of wastewater treatment, membrane fouling and membrane resistance. Fig. 1 (a) shows the conceptual structure of the model. The biological model simulates the biological treatment of wastewater based on Activated Sludge Model 1 (ASM1). The biopolymer kinetics of membrane foulants, EPS and SMP are introduced into the biological model and the ASM1 kinetics are modified by introducing the effects of transformation of SMP and growth and decay of EPS. The SMP is analyzed under two sub categories namely biomass associated products (BAP) and utilization associated products (UAP) in the biological model. In the physical model, the cake layer formation, membrane resistance and COD removal by the membrane are simulated.

Mathematical modeling and computer simulations have become useful methods for testing the efficacy of each wastewater treatment process. By using advanced software (WEST, GPS-x, SIMBA, AQUASIM, etc.), it is possible to develop a model of a full-scale wastewater treatment plant to run a simulation and, interpret the results under various operating conditions (Łagód et al., 2019). Since the models consist of a set of non-linear ordinary differential equations, the solution requires the use of numerical solvers to compute the model outputs. There are several commercial software tools available that include numerical solvers as well as a suite of implemented ASM models and models dedicated to MBR systems. In this study, AQUASIM platform was selected for the modelling (Reichert, 1994, 1998).

2.1. Biological model

The major biological component of the MBR is the activated sludge system, which is the core of the model as well. The modern age of wastewater treatment modeling started with the publication of ASM1 (Henze et al., 1987) followed by ASM2, ASM2d, ASM3 (Henze et al., 2000) and Anaerobic Digestion Model (Batstone et al., 2002). The International Water Association's (IWA) introduction of the ASM model family was critical in providing a standardized set of basis for the activated sludge models. The biological model constructed in this study is based on ASM1.

In addition to ASM1, the biopolymer kinetics in terms of growth and hydrolysis of SMP and EPS should be included in the biological model to relate their effects on membrane fouling and the performance of the physical model. Variables considered in the biological model can be categorized into two types, one as wastewater characteristics and the other as fouling associated products. The wastewater characteristics can be further divided into three groups as carbonaceous, nitrogenous and other materials. Carbonaceous material consist of soluble inert organic matter (which are not consumed within the system and do not react within the system), particulate inert organic matter (which do not react but are being produced during the biomass decay), readily biodegradable substrate (which is consumed rapidly as it is directly available for microorganisms) and produced in the system by hydrolysis of biodegradable particulate fraction, slowly biodegradable substrate and autotrophic and heterotrophic biomass. Nitrogenous material consist of NH_4^+ and NH_3 nitrogen, nitrate and nitrite nitrogen, soluble biodegradable organic nitrogen, particulate biodegradable organic nitrogen and nitrogen.

The biopolymer characteristics are considered in two types namely EPS and SMP. Formation of bound EPS is growth associated. EPS are described by the concentration of extracellular polymeric substances (X_{EPS}). Production of EPS is described by expression 13 (Janus and Ulanicki, 2015). SMPs are defined as the soluble cellular components that are released to the system during cell lysis (Jiang et al., 2008; Teng et al., 2019). The processes responsible for the formation of SMP are substrate utilization, biomass decay and EPS hydrolysis (Shi et al., 2018). Zhang et al. (2020) presented SMP as UAP and BAP. UAP is controlled by specific substrate utilization rate. BAP is independent of

Table 1
Nomenclature of variables used in the biological model.

Symbol	Description	Units
State variables		
S_I	Soluble inert organic matter	g COD m^{-3}
S_S	Readily biodegradable substrate	g COD m^{-3}
S_O	Dissolved oxygen	g O_2 m^{-3}
S_{NO}	Nitrate and nitrite nitrogen	g N m^{-3}
S_{N2}	Dinitrogen	g N m^{-3}
S_{NH}	NH_4^+ and NH_3 nitrogen	g N m^{-3}
S_{ND}	Soluble biodegradable organic nitrogen	g N m^{-3}
S_{ALK}	Alkalinity	mole HCO_3^- m^{-3}
X_A	Autotrophic biomass	g COD m^{-3}
X_H	Heterotrophic biomass	g COD m^{-3}
X_I	Particulate inert organic matter	g COD m^{-3}
X_P	Particulate products arising from biomass decay	g COD m^{-3}
X_S	Slowly biodegradable substrate	g COD m^{-3}
X_{ND}	Particulate biodegradable organic nitrogen	g N m^{-3}
S_{UAP}	Utilization associated products	g COD m^{-3}
S_{BAP}	Biomass associated products	g COD m^{-3}
X_{EPS}	Extracellular polymeric substances	g COD m^{-3}
Kinetic Parameters		
$\mu_{H,20}$	Maximum specific growth rate of heterotrophic biomass	d^{-1}
$\mu_{A,20}$	Maximum specific growth rate of autotrophic biomass	d^{-1}
$b_{H,20}$	Decay rate for heterotrophic biomass	d^{-1}
$b_{A,20}$	Decay rate for autotrophic biomass	d^{-1}
$k_{a,20}$	Maximum specific ammonification rate	d^{-1}
$k_{h,20}$	Maximum specific hydrolysis rate	d^{-1}
$\mu_{BAP,20}$	Maximum specific growth rate of heterotrophs on S_{BAP}	d^{-1}
$\mu_{UAP,20}$	Maximum specific growth rate of heterotrophs on S_{UAP}	d^{-1}
$k_{h,EPS,20}$	Maximum XEPS hydrolysis rate	d^{-1}
Stoichiometric parameters		
$K_{X,20}$	Half saturation coefficient for hydrolysis of organic compounds	–
K_{OH}	Half saturation coefficient for oxygen in heterotrophic growth	g O_2 m^{-3}
K_S	Half saturation coefficient for substrate in heterotrophic growth	g COD m^{-3}
K_{NO}	Half saturation coefficient for NO_3^- in heterotrophic growth	g N m^{-3}
K_{NH}	Half saturation coefficient for ammoniacal N in autotrophic growth	g N m^{-3}
K_{OA}	Half saturation coefficient for oxygen in autotrophic growth	g O_2 m^{-3}
Δ_h	Correction factor for hydrolysis under anoxic conditions	–
Δ_g	Correction factor for μ_H under anoxic conditions	–
K_{ALKH}	Half saturation coefficient for alkalinity (HCO_3^-) in heterotrophic growth	
K_{ALKA}	Half saturation coefficient for alkalinity (HCO_3^-) in autotrophic growth	
Y_H	Yield coefficient for heterotrophic biomass	g COD g COD^{-1}
Y_A	Yield coefficient for autotrophic biomass	g COD g COD^{-1}
i_{XB}	N content of biomass	g N g COD^{-1}
i_{XP}	N content of products of biomass decay	g N g COD^{-1}
f_P	Fraction of biomass leading to particulate products	g COD g COD^{-1}
K_{BAP}	Half saturation constant for S_{BAP}	g COD m^{-3}
K_{UAP}	Half saturation constant for S_{UAP}	g COD m^{-3}
Y_{SMP}	Yield coefficient for heterotrophic growth on SMP	g COD g COD^{-1}
γ_H	Fraction of S_{UAP} produced during heterotrophic growth	g COD g COD^{-1}
γ_A	Fraction of S_{UAP} produced during autotrophic growth	g COD g COD^{-1}
i_{XBAP}	N content of S_{BAP}	g N g COD^{-1}
i_{XEPS}	N content of X_{EPS}	g N g COD^{-1}
f_S	Fraction of S_S produced from X_{EPS} hydrolysis	g COD g COD^{-1}
$f_{EPS,dh}$	Fraction of X_{EPS} produced from heterotrophic biomass decay	g COD g COD^{-1}
$f_{EPS,da}$	Fraction of X_{EPS} produced from autotrophic biomass decay	g COD g COD^{-1}
$f_{EPS,h}$	Fraction of X_{EPS} produced from heterotrophic biomass activity	g COD g COD^{-1}
$f_{EPS,a}$	Fraction of X_{EPS} produced from autotrophic biomass activity	g COD g COD^{-1}
f_{BAP}	Fraction of S_{BAP} produced from biomass decay	

the cell growth rate and it is controlled by the cell concentration. Table 1 shows the variables used in the biological model. Variables include state variables (whose concentrations change with time) which depict the wastewater characteristics, stoichiometric parameters and parameters used to define reaction rates. The Peterson's matrix in Table 2 illustrates the relationships of processes and variables through stoichiometric parameters. The reaction rate expressions for each process are listed below.

Aerobic growth of heterotrophs:

$$\mu_{H,20}e^{-0.069(20-T)}\frac{S_S}{K_S+S_S}\frac{S_O}{K_{OH}+S_O}\frac{S_{ALK}}{K_{ALKH}+S_{ALK}}X_H \quad (1)$$

Anoxic growth of heterotrophs:

$$\mu_{H,20}e^{-0.069(20-T)}\eta_g\frac{S_S}{K_S+S_S}\frac{S_O}{K_{OH}+S_O}\frac{S_{NO}}{K_{NO}+S_{NO}}\frac{S_{ALK}}{K_{ALKH}+S_{ALK}}X_H \quad (2)$$

Hydrolysis of heterotrophs:

$$b_{H,20}e^{-0.11(20-T)}X_H \quad (3)$$

Aerobic growth of autotrophs:

$$\mu_{A,20}e^{-0.098(20-T)}\frac{S_{NH}}{K_{NH}+S_{NH}}\frac{S_O}{K_{OA}+S_O}\frac{S_{ALK}}{K_{ALKH}+S_{ALK}}X_H \quad (4)$$

Hydrolysis of autotrophs:

$$b_{A,20}e^{-0.098(20-T)}X_A \quad (5)$$

Ammonification:

$$k_{a,20}e^{-0.069(20-T)}S_{ND}X_H \quad (6)$$

Hydrolysis of organic nitrogen:

$$k_{h,20}e^{-0.11(20-T)}\frac{\frac{X_S}{X_H}}{K_{X20e^{-0.11(20-T)}}+\frac{X_S}{X_H}}\left(\frac{S_O}{K_{OH}+S_O}+\eta_h\frac{K_{OH}}{K_{OH}+S_O}\frac{S_{NO}}{K_{NO}+S_{NO}}+\eta_h\frac{K_{Oan}}{K_{Oan}+S_O+S_{NO}}\right)X_H\frac{X_{ND}}{X_S} \quad (7)$$

Hydrolysis of organics:

$$k_{h,20}e^{-0.11(20-T)}\frac{\frac{X_S}{X_H}}{K_{X20e^{-0.11(20-T)}}+\frac{X_S}{X_H}}\left(\frac{S_O}{K_{OH}+S_O}+\eta_h\frac{K_{OH}}{K_{OH}+S_O}\frac{S_{NO}}{K_{NO}+S_{NO}}+\eta_h\frac{K_{Oan}}{K_{Oan}+S_O+S_{NO}}\right)X_H \quad (8)$$

Aerobic growth of S_{BAP}:

$$\mu_{BAP,20}e^{-0.069(20-T)}\frac{S_{BAP}}{K_{BAP}+S_{BAP}}\frac{S_O}{K_{OH}+S_O}\frac{S_{ALK}}{K_{ALKH}+S_{ALK}}X_H \quad (9)$$

Anoxic growth of S_{BAP}:

$$\mu_{BAP,20}e^{-0.069(20-T)}\eta_g\frac{S_{BAP}}{K_{BAP}+S_{BAP}}\frac{S_O}{K_{OH}+S_O}\frac{S_{NO}}{K_{NO}+S_{NO}}\frac{S_{ALK}}{K_{ALKH}+S_{ALK}}X_H \quad (10)$$

Aerobic growth on S_{UAP}:

$$\mu_{UAP,20}e^{-0.069(20-T)}\frac{S_{UAP}}{K_{UAP}+S_{UAP}}\frac{S_O}{K_{OH}+S_O}\frac{S_{ALK}}{K_{ALKH}+S_{ALK}}X_H \quad (11)$$

Anoxic growth on S_{UAP}:

Table 2
Peterson's Matrix of ASM1 and Biopolymer kinetics for the combined model.

index	1	2	3	4	5	6	7	8	9	10	11	12	13	14	15	16	17
Process	S_r	S_s	X_I	X_s	$X_{B,H}$	$X_{B,A}$	X_P	S_O	S_{NO}	S_{N2}	S_{NH}	S_{ND}	X_{ND}	S_{ALK}	X_{EPS}	S_{UAP}	S_{BAP}
Aerobic growth of heterotrophs		$-\frac{1}{Y_H}$			$1-f_{EPS,h}$			$-\frac{1-Y_H-\gamma_H}{Y_H}$			y_{2a}			$-\frac{i_{XB}}{14}$	$f_{EPS,h}$	$\frac{\gamma_H}{Y_A}$	
Anoxic growth of heterotrophs		$-\frac{1}{Y_H}$			$1-f_{EPS,h}$				$-\frac{1-Y_H-\gamma_H}{2.86Y_H}$	$\frac{1-Y_H-\gamma_H}{2.86Y_H}$	y_{2a}			$\frac{1-Y_H}{14*2.86Y_H}-\frac{i_{XB}}{14}$	$f_{EPS,h}$	$\frac{\gamma_H}{Y_H}$	
Aerobic growth of autotrophs						$1-f_{EPS,a}$		$-\frac{4.57-Y_A}{Y_A}$	$\frac{1}{Y_A}$		$-i_{XB}-\frac{1}{Y_A}$			$-\frac{i_{XB}}{14}-\frac{1}{7Y_A}$	$f_{EPS,a}$	$\frac{\gamma_A}{Y_A}$	
Decay of heterotrophs				$1-f_p-f_{EPS,dh}-f_{BAP}$	-1		f_p						$-i_{XP}-f_p*i_{XP}$		$f_{EPS,h}$		f_{BAP}
Decay of autotrophs				$1-f_p-f_{EPS,da}-f_{BAP}$		-1	f_p						$-i_{XP}-f_p*i_{XP}$		$f_{EPS,da}$		f_{BAP}
Ammonification of soluble organic nitrogen											1	-1		$\frac{1}{14}$			
Hydrolysis' of entrapped organics		1		-1													
Hydrolysis' of entrapped organic nitrogen												1	-1				
Aerobic growth of S_{BAP}					$1-f_{EPS,h}$			$-\frac{1-Y_{SMP}}{Y_{SMP}}$			y_{2b}			$-\frac{i_{XB}}{14}$	$f_{EPS,h}$		$-\frac{1}{Y_{SMP}}$
Anoxic growth of S_{BAP}					$1-f_{EPS,h}$				$-\frac{1-Y_{SMP}}{2.86*Y_{SMP}}$	$\frac{1-Y_{SMP}}{2.86*Y_{SMP}}$	y_{2b}			$\frac{1-Y_H}{14*2.86Y_H}-\frac{i_{XB}}{14}$	$f_{EPS,h}$		$-\frac{1}{Y_{SMP}}$
Aerobic growth on S_{UAP}					$1-f_{EPS,h}$			$-\frac{1-Y_{SMP}}{Y_{SMP}}$			y_{2a}			$-\frac{i_{XB}}{14}$	$f_{EPS,h}$	$-\frac{1}{Y_{SMP}}$	
Anoxic growth on S_{UAP}					$1-f_{EPS,h}$				$-\frac{1-Y_{SMP}}{2.86*Y_{SMP}}$	$\frac{1-Y_{SMP}}{2.86*Y_{SMP}}$	y_{2a}			$\frac{1-Y_H}{14*2.86Y_H}-\frac{i_{XB}}{14}$	$f_{EPS,h}$	$-\frac{1}{Y_{SMP}}$	
Hydrolysis of X_{EPS}		f_S													-1		$1-f_S$

$y_{2a} = -(1-f_{EPS,h})*i_{XB}-f_{EPS,h}*i_{XEPS}$

$y_{2b} = -(1-f_{EPS,h})*i_{XB}-f_{EPS,h}*i_{XEPS}+\frac{1}{Y_{SMP}}*i_{XBAP}$

$$\mu_{UAP,20} e^{-0.069(20-T)} \eta_g \frac{S_{UAP}}{K_{UAP}+S_{UAP}} \frac{S_O}{K_{OH}+S_O} \frac{S_{NO}}{K_{NO}+S_{NO}} \frac{S_{ALK}}{K_{ALKH}+S_{ALK}} X_H \quad (12)$$

Hydrolysis of X_{EPS}:

$$k_{h,EPS,20} e^{-0.11(20-T)} X_{EPS} \quad (13)$$

2.2. Physical model

The physical model simulates the main physical phenomena that occur in the membrane and influence the biological model directly or indirectly. Thus, the physical model consists of cake layer formation during membrane filtration, organic matter removal by the membrane, and membrane fouling.

2.3. Membrane fouling

Membrane fouling is considered as the main barrier for the use of MBR. As this leads to higher energy consumption and higher operating cost, it is one the most acute problems in using membranes. Membrane fouling can be defined as the coating of the membrane surface or blocking of the pores with a solid or gelatinous material, which creates a barrier through which the permeate must pass. Thus, the effective pore size of the membrane is reduced due to fouling. This will result in an increase in the hydraulic resistance of the membrane. Membrane fouling causes a decrease in permeate flux or an increase in the TMP of the MBR (Navaratna and Jegatheesan, 2011).

Membrane flux in MBRs can be influenced by concentration polarization, external fouling, and internal fouling depending on where the foulant is located relative to the membrane structure (Judd, 2010). Concentration polarization (CP) is defined as an accumulation of solutes or particles in a thin liquid layer adjacent to the outer surface of the membrane (Luis, 2018), which is an inherent phenomenon of membrane filtration. CP can reduce permeate flux by increasing the resistance to liquid flow. External fouling is caused by the deposition of particles, colloids, and macromolecules on membrane surfaces. External fouling can be divided into two types of fouling as cake fouling and gel fouling. Cake fouling is caused by the accumulation of retained solids on the membrane. Gel fouling is caused by the accumulation of soluble products and colloids. Adsorption and deposition of solutes and fine particles inside the internal pore structure of membranes cause the internal fouling (Wang et al., 2014).

EPS and SMP are the major foulants, which are a matrix of high molecular weight molecules excreted by cells (Gkotsis et al., 2014). Functions of EPS include bacterial cell aggregation in flocs and biofilms, formation of a protective barrier around the bacteria, water retention, and adhesion to surfaces. EPS can form a highly hydrated gel matrix in which microbial cells can be embedded, assisting in the formation of a significant barrier to permeate flow in membrane processes. SMP moves into the pores of the membrane causing pore blocking. Further, the type of fouling can be identified under three different categories: (i) Reversible fouling - fouling that can be removed by physical processes such as backflushing or relaxation under cross flow conditions, (ii) Irreversible fouling - fouling which can be removed by chemical cleaning, and (iii) Irrecoverable fouling - cannot be removed by any cleaning and occurs over long periods of operation (Drews, 2010).

2.4. Cake layer formation and membrane fouling

The permeate flux of a membrane is governed by the basic membrane filtration equation,

$$J = \frac{\Delta P}{\mu R_t} \quad (14)$$

Where, J = Permeate flux, ΔP = Transmembrane pressure, μ = Dynamic permeate viscosity, R_t = Total membrane resistance

The total membrane resistance, according to the classical resistance in series model, includes four parts,

$$R_t = R_m + R_i + R_r + R_p \quad (15)$$

Where, R_m = Intrinsic membrane resistance, R_r = Reversible resistance from cake layer, R_i = Irrecoverable resistance, R_p = Irreversible resistance due to pore blocking which can be recovered by chemical cleaning.

The time-dependent resistance resulting from reversible fouling,R_r, can be expressed as

$$R_r = \alpha m_r \quad (16)$$

Where, α = specific resistance of reversible fouling, m_r = amount of reversible foulants, and $m_r$can be expressed as,

$$\frac{dm_r}{dt} = JX_T - k_r m_r \quad (17)$$

Where, k_r = detachment coefficient to account for cross flow, X_T = MLSS concentration.

Irreversible resistance, R_p due to pore blocking is given by

$$R_p = k_p m_p \quad (18)$$

Where, m_p = amount of reversible foulants causing pore blocking, k_p = fouling strength of SMP in pore blocking and m_p can be expressed as,

$$\frac{dm_p}{dt} = \beta J S_{SMP} \quad (19)$$

where, β = fraction of SMP causing pore blocking, S_{SMP} = Concentration of SMP.

Irrecoverable fouling, R_i is given by:

$$R_i = k_i m_i \quad (20)$$

Where, m_i = amount of irreversible foulants, k_i = fouling strength of SMP for irreversible fouling and m_i can be expressed as,

$$\frac{dm_i}{dt} = bJS_{SMP} \quad (21)$$

where, b = fraction of SMP causing irreversible fouling.

2.5. Physical and chemical cleaning

In conventional pressure driven water filtration, the flux is fixed and appropriate TMP is maintained (Judd, 2010). The main impact of the operating flux is on the cleaning frequency, which may be by physical or chemical means. Physical cleaning is generally achieved by backflushing or relaxation with continuous air scouring. Chemical cleaning can be performed in two ways as chemically enhanced backflushing which can be performed frequently and chemical cleaning which can be performed periodically. The physical cleaning removes the solids attached onto the membrane surface. These solid particles are termed as reversible foulants. The chemical cleaning removes irreversible foulants leaving irrecoverable foulants on the membrane and inside membrane pores.

2.6. MBR model construction in AQUASIM

AQUASIM modelling system was chosen to develop the model for MBR. AQUASIM is a “computer program for the identification and simulation of aquatic systems” developed by Swiss Federal Institute for Environmental Science and Technology (EAWAG) (Reichert, 1998). The model comprises a set of ordinary and/or partial differential equations and algebraic equations that describe the behavior of a given set of

important state variables in an aquatic system in a deterministic manner. The differential equations for processes can be utilized in compartments, which can be connected by links. Main elements of the model structure consist of variables, processes, compartments and links.

For the modelling of the integrated MBR system, the state variables, kinetic parameters and stoichiometric parameters given in Table 1 were defined initially. The processes discussed above were related to variables with stoichiometric coefficients using Peterson's matrix (Table 2). Fig. 1(b) shows the compartments and links used for the integrated model developed to simulate the MBR in AQUASIM. Wastewater is fed to the initial anoxic reactor. Variables representing wastewater characteristics, biopolymer characteristics, activated sludge processes and processes related to EPS and transformation of SMP were activated in the anoxic reactor compartment defined in the model that had been constructed in AQUASIM. The overflow from the anoxic reactor compartment reaches the aerobic reactor compartment where the variables and processes simulated in the anoxic reactor were replicated. New process to aerate the reactor is used in the aerobic reactor compartment. The physical model system with the membrane module is used within the aerobic reactor compartment to simulate the physical separation and membrane fouling phenomena.

Filtration mechanism is simulated using substance separation. A dummy compartment named Overflow Tank (Fig. 1(b)) was used and linked to Aerobic MBR Tank. From the link between the MBR and overflow tank, a bifurcation was used where substance flow can be controlled. The membrane filtration is simulated by controlling the particulate matter transferring through this bifurcation to the effluent. Thus only the soluble matter is allowed to pass through the virtual membrane to the permeate side. Another bifurcation from MBR-Overflow link is used to introduce recirculation between aerobic MBR tank and the anoxic rector. In this link, all the matter is allowed to pass through. The state variables representing the amount of foulants attached to membrane surfaces are defined as surface variables. These variables are activated in the aerobic MBR tank simulating the membrane fouling processes described in equations (17), (19) and (21) and membrane resistance with relation to biopolymer concentrations described by equations (14)–(16) and (18) and (20). The volumes of the tanks and flow rates can be defined based on the conditions requiring simulation.

For the model calibration, data reported in the experiments performed by Di Bella et al. (2010) on submerged MBR were used. The study consisted of two phases where in the first phase, the pilot plant was started without introducing activated sludge and without sludge removal. In the second phase the MBR pilot plant was started with the introduction of activated sludge and the sludge was removed continuously to maintain a constant sludge concentration. The first phase of the study was used for the model calibration and the second phase was used for the validation of the calibrated model.

The pilot plant reported in Di Bella et al. (2010) consisted of an aerobic MBR tank with a volume of 0.190 m^3. Hollow fiber Zenon ZW10 membrane module was submerged into the reactor and permeate was pumped out to a permeate tank. In both phases of the experiment, a hydraulic retention time of 10 h had been used with a flow rate of 190 L/h (0.456 m^3/day). The membrane module has been operated with constant flux rate of 21 L/m^2/h (0.504 m/day).

In phase 1, which was used for the calibration of the model, wastewater with average COD concentration of 527 mg/L, average NH_4^+–N concentration of 48 mg/L, TSS of 294 mg/L have been reported. The COD fractions have been identified as, 15% of S_s, 6% of S_i, 32% of X_s, 42% of X_i, and 5% of active biomass. The system has been operated for 65 days with the above conditions and COD, NH_4^+–N and NO_3^- concentrations have been measured. The MLSS concentration in the aerobic MBR tank and the TMP across the membrane have been measured and reported. These measured values were used to calibrate the model. In phase 2 of the experiment, a SRT of 35 days has been used with initial MLSS concentration of 13.4 g/L. The reported values for phase 2 were used in validating the model.

The physical and chemical cleaning of the reactors is simulated by removing a portion of foulants attached on to membrane module. In physical cleaning, the reversible foulants attached are removed and in chemical cleaning, reversible pore blocking foulants are removed. This phenomenon is simulated by identifying the cleaning frequency using a variable and once the time reached the cleaning cycle, the foulants attached are reduced.

The experiments of Di Bella et al. (2010) has not used frequent cleaning of the membrane module. In order to check the effect of the frequent cleaning of the membranes in the developed model, another data set from an experiment by Nagaoka et al. (1998) was used. A laboratory scale experiment has been conducted to identify the biofouling in a submerged MBR. Tank of 28 L volume has been used as the aerobic reactor and the wastewater has been fed with organic loading rate of 1.5 g/L.day. A membrane module with a total surface area of 0.273 m^2 has been submerged in the aerobic reactor to complete the MBR. Constant permeate flux of 0.15 m^3/m^2.day has been used for permeating. Once the permeate flow rate has started to drop with the increase in TMP, the membrane module has been cleaned physically.

3. Results and discussion

3.1. Model calibration

Determining all model parameters is a tedious process. Henze et al. (2000) suggested using reported default values from previous applications in modelling. A sensitivity analysis can be performed to identify the most sensitive and relatively less sensitive parameters (Shokrkar et al., 2018). Determination of optimal values of the parameters of selected model using the measured data with the aid of parameter estimation procedure was performed to assign the sensitive parameters with calibrated values.

3.1.1. Sensitivity analysis

The MBR model constructed in this study consists of 49 parameters and 17 state variables. The state variables discussed in the model were lumped into categories in terms of TSS, COD, TKN and TN using equations (22)–(25) respectively.

$$COD = S_S + S_I + X_S + X_H + X_A + X_P + X_I + X_{EPS} + S_{SMP} \quad (22)$$

$$TSS = 0.75(X_S + X_H + X_A + X_P + X_I + X_{EPS}) \quad (23)$$

$$TKN = S_{NH} + S_{NO} + X_{ND} + i_{XB}(X_H + X_A) + i_{XP}(X_P + X_I) + i_{XBAP} S_{BAP} + i_{XEPS} X_{EPS} \quad (24)$$

$$TN = TKN + S_{NO} \quad (25)$$

A total of 49 influencing parameters were considered and the sensitivity of each parameter on the considered variables was analyzed. The results of sensitivity analysis can be found in supplementary materials. The sensitivity analysis allows quantifying the influence of parameters on the variables. $\mu_{A,20}$, $\mu_{H,20}$, $b_{H,20}$, $b_{A,20}$, $f_{EPS,h}$, $f_{EPS,a}$, K_{OA}, K_S, K_{ALKH}, Y_H, Y_A, K_{UAP}, η_g, K_{NH}, γ_A, α, k_i, k_p, a, b and c were identified as the sensitive parameters with high impact on variables lumped as COD, MLSS, TN, total membrane resistance and TMP. Based on the sensitivity analysis, $\mu_{A,20}$, $\mu_{H,20}$, $b_{H,20}$ and $b_{A,20}$ seemed to have higher influence on each variable considered.

3.1.2. Parameter estimation

Model calibration was performed using experimental data of phase 1 experiments reported in Di Bella et al. (2010). Values of sensitive parameters were estimated during parameter estimation and others were given with values obtained from literature. The calibrated values for kinematic and stoichiometric parameters used in the model are given in

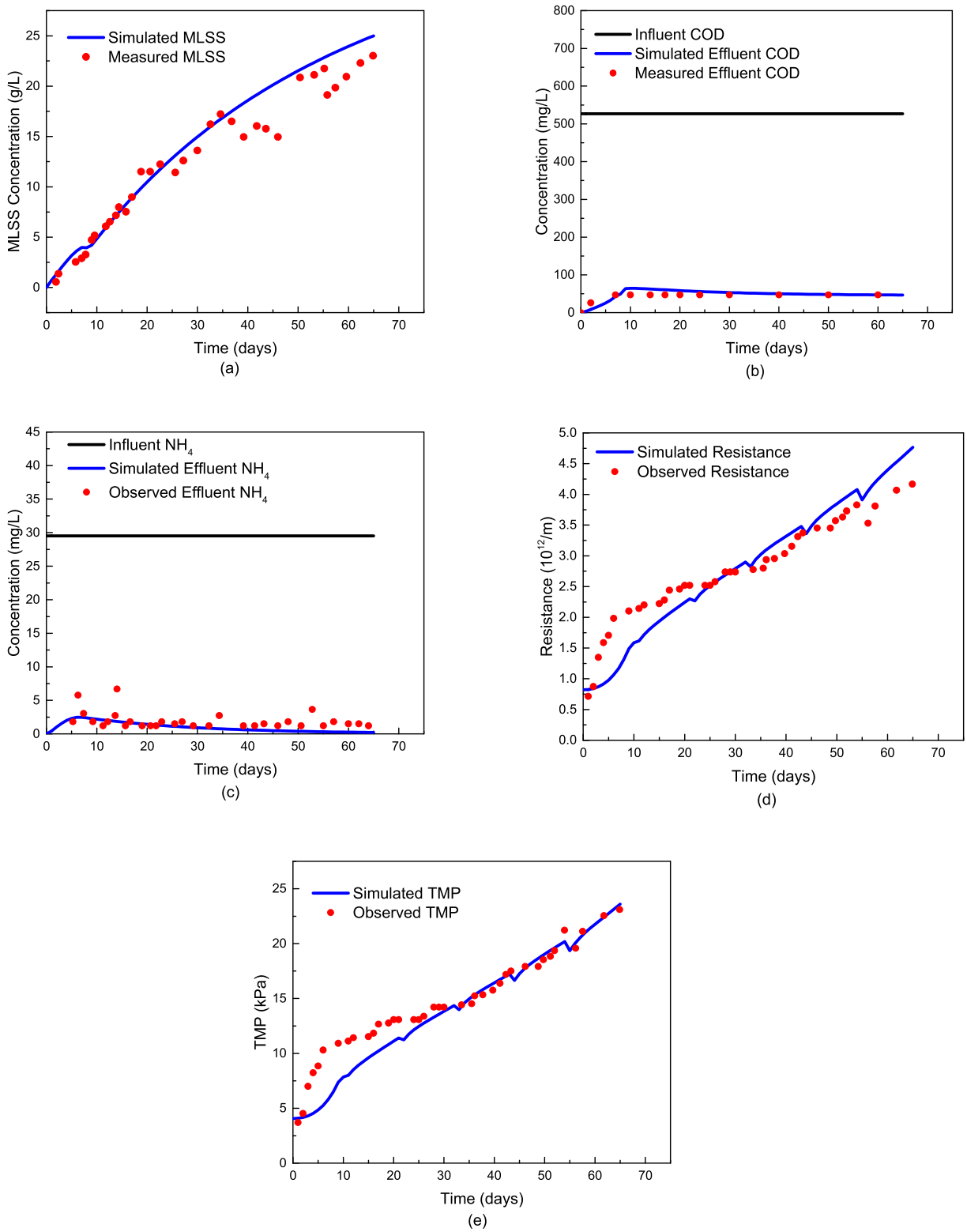

Fig. 2. Comparison of observed and simulated values of (a) MLSS in the aerobic MBR tank, (b) COD, (c) NH_4^+–N, (d) total membrane resistance and (e) TMP.

supplementary materials. In general, the parameters estimated in this study were consistent with data reported in the literature.

With calibration of the model, the simulated values of MLSS, COD, NH_4^+-N, R_t and TMP were compared with those reported from the experiment. Fig. 2 shows the comparisons of MLSS, COD, NH_4^+–N, resistance and TMP. A good prediction could be observed with respect to long term simulation of the model despite some disagreements observed in values of membrane resistance and TMP during the first 20 days of simulation. Further comparison was made using the root mean square error (RMSE), mean absolute error (MAE) and correlation coefficient (R^2) to provide quantitative assessment on the performance of the model. The reported and simulated values resulted in RMSE of 1.95, 10.95, 1.46, 0.47 and 1.79 for MLSS, COD, NH_4^+–N, resistance and TMP respectively. This shows that the calibration of the model

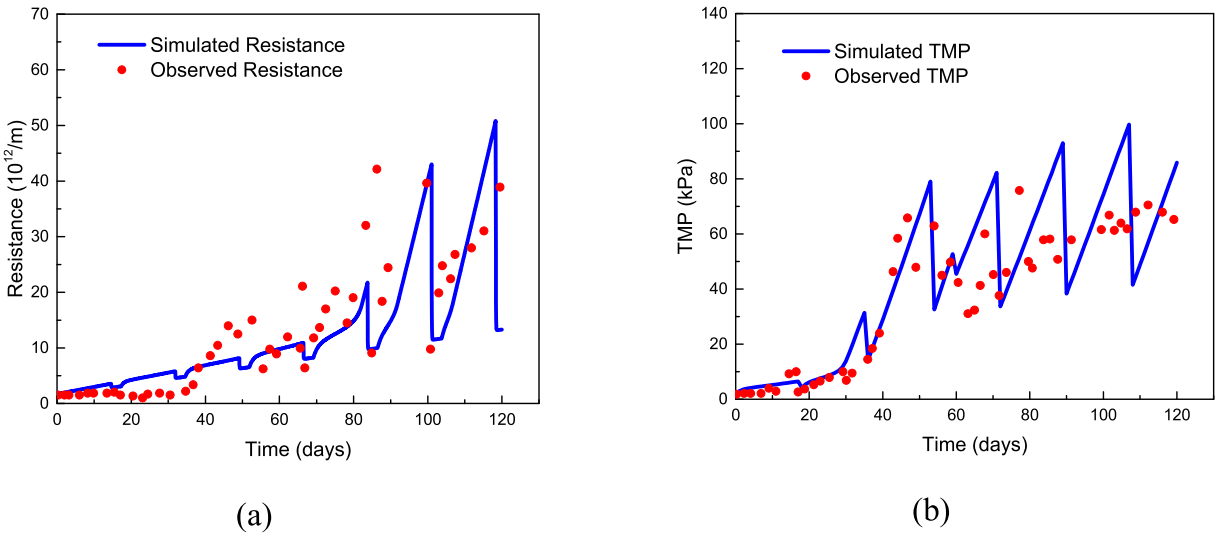

Fig. 3. Comparison of observed and simulated values of (a) total membrane resistance and (b) TMP.

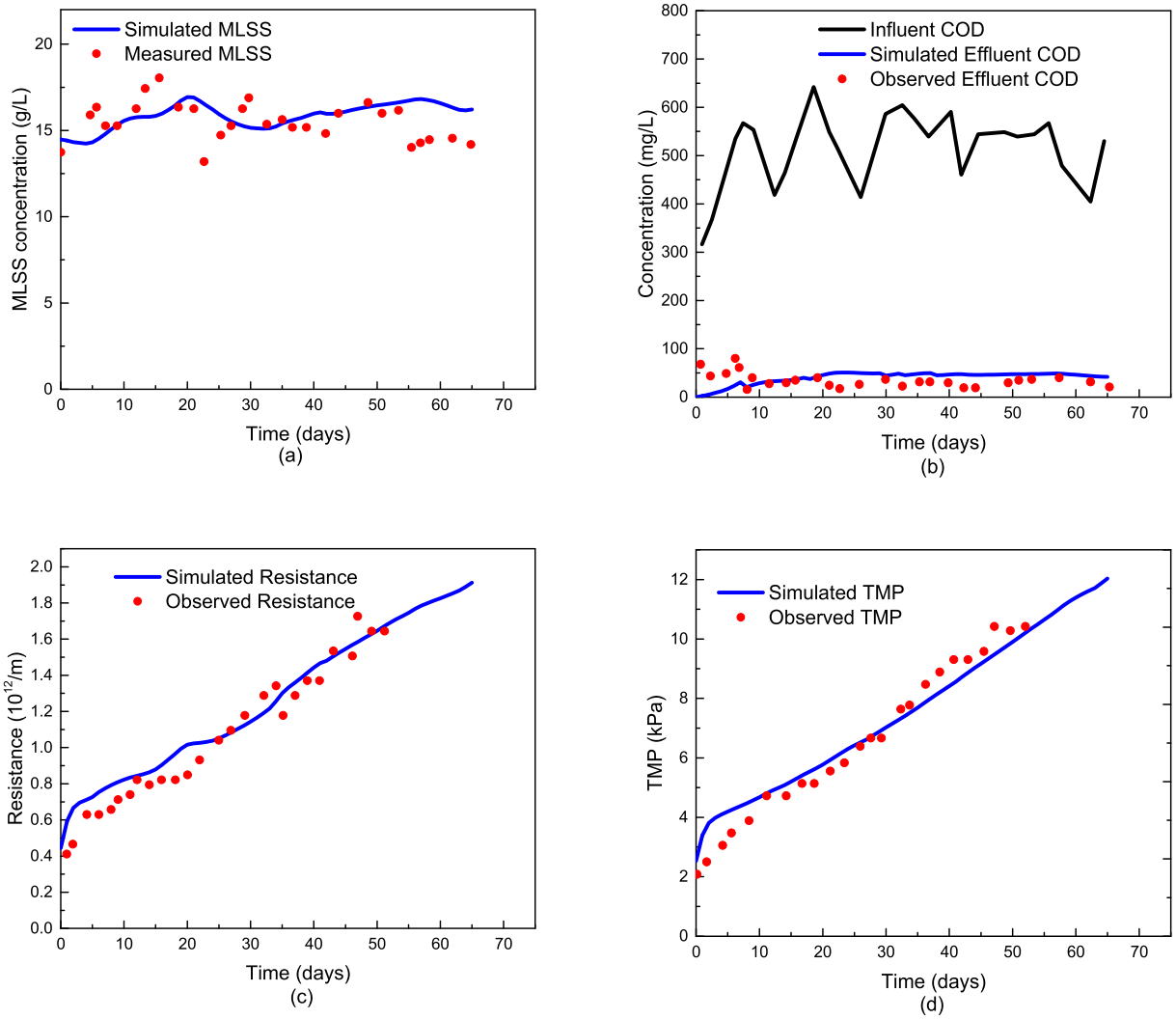

Fig. 4. Comparison of the modelled and simulated values for validation of the model (a) MLSS in the aerobic MBR tank, (b) COD, (c) total membrane esistance and (d) TMP.

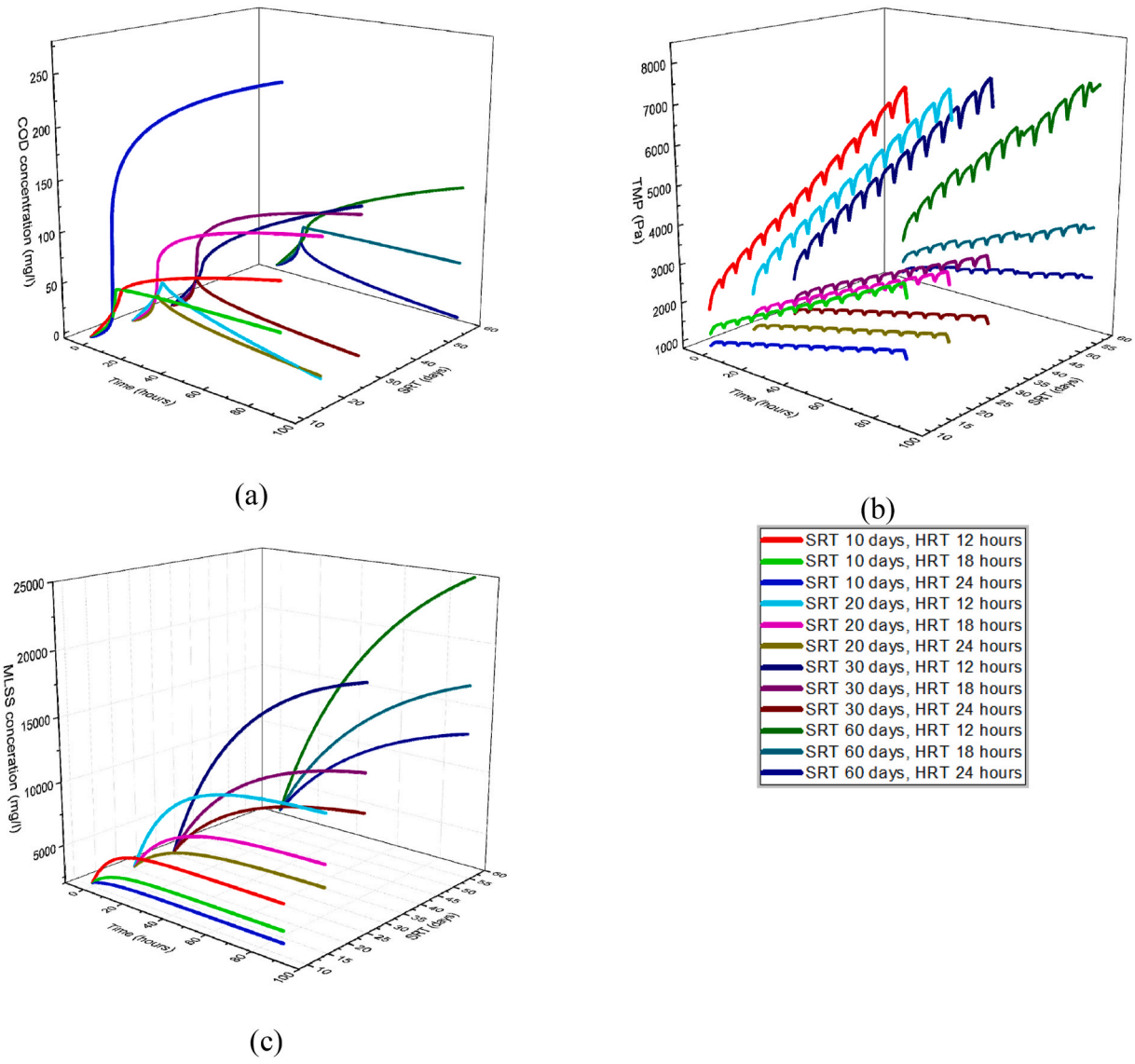

Fig. 5. Results from the simulation of calibrated and validated model for different operating conditions (a) COD concentration in the effluent, (b) TMP, (c) MLSS in the aerobic MBR tank.

with respect to the parameters considered is satisfying. Further the MAE also found to be in acceptable range for MLSS, COD, NH_4–N, resistance and TMP with values of 0.11, 0.20, 0.52, 0.14 and 0.09 respectively. The R^2 values found to be 0.97, 0.82, 0.15, 0.94 and 0.95 respectively for MLSS, COD, NH_4–N, resistance and TMP. From MAE and R^2 for NH_4–N, the model results seem slightly off from the observed value with other parameters show acceptable comparisons.

The physical and chemical cleaning of the membrane module is simulated in the model with reference to experiments reported by Nagaoka et al. (1998). The comparison of the modelled and simulated values of TMP and resistance with frequent cleaning are shown in Fig. 3. Comparing the values using statistical measures, $R^2 = 0.60$ for the resistance and $R^2 = 0.75$ for TMP showing that the calibration is acceptable.

3.2. Model validation

For the validation of the model, second phase of the experiments reported by (Di Bella et al., 2010) was used (the details of experiments have been given in section 2.4). Fig. 4 shows the comparison of simulated results with the observed values in the experiment. The system was initiated with MLSS concentration of 13.4 g/L. The model simulated the conditions accurately by yielding a similar pattern on the change in MLSS concentration over the duration of 65 days of simulation as depicted in Fig. 4(a). The RMSE of MLSS values was 1.42 and MAE was 0.07. The COD was fed as reported and the range of COD in the effluent of the model was in the range of that of experiments with RMSE of 109.71 and MAE of 0.61. Fig. 4 (c) and (d) show the variation of the total membrane resistance and the TMP over time. The variation in resistance and TMP predicted by the model were in agreement with the reported values of the experiment with RMSE of 0.16 and 0.66 and MAE of 0.13 and 0.08, respectively. These observations indicate that the calibrated model performs well and is valid. The calibrated and validated model can be used to predict the performance of MBR under different conditions.

3.3. Simulation of MBR performance under different operating conditions

The calibrated and validated model was used to simulate different SRTs and HRTs to identify and predict the performance of a MBR. An initial MLSS concentration of 3,050 g/L was used in the simulations. The COD in the influent was kept at 500 mg/L. SRT of 60 days, 30 days, 20

days and 10 days were simulated for HRTs of 12, 18 and 24 h. The MBR performance was analyzed with respect to COD removal and the variation of TMP as shown in Fig. 5. For higher SRTs of 20, 30 and 60 days, better COD removal was observed at high HRTs (of 18 and 24 day). In the case where SRT was 10 days, the COD removal at HRT of 24 h was considerably lower. The lower MLSS concentration resulting from lower flow rate of influent is causing this lower removal of COD (at HRT of 24 h at SRT of 10 days). The MLSS concentrations shows the obvious pattern where the lower HRT results in higher MLSS concentration for all the SRTs and with the increase in sludge age, the MLSS concentration rises. The TMP variation in the model shows that the TMP is less affected by the sludge age and the increase in permeate flux through the membrane with lower HRTs causes higher TMPs.

4. Conclusions

In this study, a model based on ASM1 to simulate MBR has been developed. The ASM1 was extended with the kinetics of SMP and EPS. The physical phenomena of permeate separation by membrane filtration is simulated in the physical component (model) of the integrated model. The membrane resistance is modelled as a combination of pore fouling, cake layer fouling, and irreversible fouling. The resistance is related to the concentrations of EPS and SMP. Sensitivity analysis is conducted to identify the parameters which need estimation to calibrate the model.

Once the model was calibrated it was able to predict the effluent quality of an MBR at a given HRT and SRT as well the fouling behavior of the membrane under a given frequency of regular cleaning. For example, the model showed that at higher HRTs, the COD removal by the MBR will increase with the increase in SRTs and the TMP is sensitive to HRT but not to SRT. The model also was able to predict the time required to initiate chemical cleaning of the membrane under a given operating conditions.

The model requires extensive details of wastewater characteristics including fractions of COD which are not measured commonly. In cases where the complete data sets are not available, typical values for a given wastewater could be used for simulations. Further, the calibration of the model can be done for different types of wastewater where the stoichiometric parameters of those wastewaters under different conditions can be estimated using the model. The model can be further improved by considering the fate of nutrients in the MBR. The effect of different strategies of MBR operation on the efficiency of the treatment system can be analyzed using the model.

Credit author statement

L.M.L.K.B. Lindamulla: Conceptualization, Methodology, Software, Data curation, Writing – original draft. V. Jegatheesan: Conceptualization, Methodology, Software, Supervision, Writing – review & editing, K. B.S.N. Jinadasa: Conceptualization, Supervision, Writing – review & editing, K.G.N. Nanayakkara: Conceptualization, Supervision, Writing – review & editing, M.Z. Othman: Conceptualization, Supervision, Writing – review & editing.

Declaration of competing interest

The authors declare that they have no known competing financial interests or personal relationships that could have appeared to influence the work reported in this paper.

Appendix A. Supplementary data

Supplementary data to this article can be found online at https://doi.org/10.1016/j.chemosphere.2021.131319.

References

Abdel-Fatah, M.A., 2018. Nanofiltration systems and applications in wastewater treatment. Ain Shams Engineering Journal 9, 3077–3092.

Batstone, D.J., Keller, J., Angelidaki, I., Kalyuzhnyi, S., Pavlostathis, S., Rozzi, A., Sanders, W., Siegrist, H., vavilin, V., 2002. The IWA anaerobic digestion model no 1 (ADM1). Water Sci. Technol. 45, 65–73.

Bemberis, I., 1971. Membrane Sewage Treatment Systems: Potential for Complete Wastewater Treatment. American Society of Agricultural Engineers.

Crini, G., Lichtfouse, E., 2019. Advantages and disadvantages of techniques used for wastewater treatment. Environ. Chem. Lett. 17, 145–155.

Di Bella, G., Mannina, G., Viviani, G., 2008. An integrated model for physical-biological wastewater organic removal in a submerged membrane bioreactor: model development and parameter estimation. J. Membr. Sci. 322, 1–12.

Di Bella, G., Durante, F., Torregrossa, M., Viviani, G., 2010. Start-up with or without inoculum? Analysis of an SMBR pilot plant. Desalination 260, 79–90.

Di Biase, A., Kowalski, M.S., Devlin, T.R., Oleszkiewicz, J.A., 2019. Moving bed biofilm reactor technology in municipal wastewater treatment: a review. J. Environ. Manag. 247, 849–866.

Drews, A., 2010. Membrane fouling in membrane bioreactors—characterisation, contradictions, cause and cures. J. Membr. Sci. 363, 1–28.

Du, X., Shi, Y., Jegatheesan, V., Haq, I.U., 2020. A review on the mechanism, impacts and control methods of membrane fouling in MBR system. Membranes 10, 24.

El-Fadel, M., Sleem, F., Hashisho, J., Saikaly, P., Alameddine, I., Ghanimeh, S., 2018. Impact of SRT on the performance of MBRs for the treatment of high strength landfill leachate. Waste Manag. 73, 165–180.

Gkotsis, P., Banti, D., Peleka, E., Zouboulis, A., Samaras, P., 2014. Fouling issues in membrane bioreactors (MBRs) for wastewater treatment: major mechanisms, prevention and control strategies. Processes 2, 795–866.

Gogate, P.R., Pandit, A.B., 2004. A review of imperative technologies for wastewater treatment I: oxidation technologies at ambient conditions. Adv. Environ. Res. 8, 501–551.

Hamedi, H., Ehteshami, M., Mirbagheri, S.A., Rasouli, S.A., Zendehboudi, S., 2019. Current status and future prospects of membrane bioreactors (MBRs) and fouling phenomena: a systematic review. Can. J. Chem. Eng. 97, 32–58.

Hashisho, J., El-Fadel, M., Al-Hindi, M., Salam, D., Alameddine, I., 2016. Hollow fiber vs. flat sheet MBR for the treatment of high strength stabilized landfill leachate. Waste Manag. 55, 249–256.

Henze, M., Grady, C., Gujer, W., Marais, G., Matsuo, T., 1987. Activated Sludge Model No. 1. Scientific and Technical Report No. 1. IAWPRC, London, UK.

Henze, M., Gujer, W., Mino, T., Van Loosdrecht, M.C., 2000. Activated Sludge Models ASM1, ASM2, ASM2d and ASM3. IWA publishing.

Jagaba, A., Kutty, S., Lawal, I., Abubakar, S., Hassan, I., Zubairu, I., Umaru, I., Abdurrasheed, A., Adam, A., Ghaleb, A., 2021. Sequencing batch reactor technology for landfill leachate treatment: a state-of-the-art review. J. Environ. Manag. 282, 111946.

Janus, T., 2014. Integrated mathematical model of a MBR reactor including biopolymer kinetics and membrane fouling. Procedia Engineering 70, 882–891.

Janus, T., Ulanicki, B., 2015. ASM1-based activated sludge model with biopolymer kinetics for integrated simulation of membrane bioreactors for wastewater treatment. Procedia Engineering 119, 1318–1327.

Jiang, T., Myngheer, S., De Pauw, D.J., Spanjers, H., Nopens, I., Kennedy, M.D., Amy, G., Vanrolleghem, P.A., 2008. Modelling the production and degradation of soluble microbial products (SMP) in membrane bioreactors (MBR). Water Res. 42, 4955–4964.

Judd, S., 2010. The MBR Book: Principles and Applications of Membrane Bioreactors for Water and Wastewater Treatment. Elsevier.

Le-Clech, P., Jefferson, B., Judd, S., 2005. A comparison of submerged and sidestream tubular membrane bioreactor configurations. Desalination 173, 113–122.

Luis, P., 2018. Fundamental Modeling of Membrane Systems: Membrane and Process Performance. Elsevier.

Mannina, G., Di Bella, G., Viviani, G., 2011. An integrated model for biological and physical process simulation in membrane bioreactors (MBRs). J. Membr. Sci. 376, 56–69.

Masindi, V., Muedi, K.L., 2018. Environmental contamination by heavy metals. Heavy metals 10, 115–132.

Michael, I., Rizzo, L., Mcardell, C., Manaia, C., Merlin, C., Schwartz, T., Dagot, C., Fatta-Kassinos, D., 2013. Urban wastewater treatment plants as hotspots for the release of antibiotics in the environment: a review. Water Res. 47, 957–995.

Morrow, C.P., Mcgaughey, A.L., Hiibel, S.R., Childress, A.E., 2018. Submerged or sidestream? The influence of module configuration on fouling and salinity in osmotic membrane bioreactors. J. Membr. Sci. 548, 583–592.

Nagaoka, H., Yamanishi, S., Miya, A., 1998. Modeling of biofouling by extracellular polymers in a membrane separation activated sludge system. Water Sci. Technol. 38, 497–504.

Navaratna, D., Jegatheesan, V., 2011. Implications of short and long term critical flux experiments for laboratory-scale MBR operations. Bioresour. Technol. 102, 5361–5369.

Naz, I., Saroj, D.P., Mumtaz, S., Ali, N., Ahmed, S., 2015. Assessment of biological trickling filter systems with various packing materials for improved wastewater treatment. Environ. Technol. 36, 424–434.

Reichert, P., 1994. AQUASIM-A tool for simulation and data analysis of aquatic systems. Water Sci. Technol. 30, 21.

Reichert, P., 1998. AQUASIM 2.0-User Manual. Swiss Federal Institute for Environmental Science and Technology. Dubendorf, Switzerland.

Samer, M., 2015. Biological and chemical wastewater treatment processes. Wastewater treatment engineering 150.
Shi, Y., Huang, J., Zeng, G., Gu, Y., Hu, Y., Tang, B., Zhou, J., Yang, Y., Shi, L., 2018. Evaluation of soluble microbial products (SMP) on membrane fouling in membrane bioreactors (MBRs) at the fractional and overall level: a review. Rev. Environ. Sci. Biotechnol. 17, 71–85.
Shokrkar, H., Ebrahimi, S., Zamani, M., 2018. Enzymatic hydrolysis of microalgal cellulose for bioethanol production, modeling and sensitivity analysis. Fuel 228, 30–38.
Teng, J., Zhang, M., Leung, K.-T., Chen, J., Hong, H., Lin, H., Liao, B.-Q., 2019. A unified thermodynamic mechanism underlying fouling behaviors of soluble microbial products (SMPs) in a membrane bioreactor. Water Res. 149, 477–487.
Wang, Z., Ma, J., Tang, C.Y., Kimura, K., Wang, Q., Han, X., 2014. Membrane cleaning in membrane bioreactors: a review. J. Membr. Sci. 468, 276–307.
Wang, J., Cahyadi, A., Wu, B., Pee, W., Fane, A.G., Chew, J.W., 2020. The roles of particles in enhancing membrane filtration: a review. J. Membr. Sci. 595, 117570.
Waqas, S., Bilad, M.R., 2019. A review on rotating biological contactors. Indonesian Journal of Science and Technology 4, 241–256.
Zarragoitia-González, A., Schetrite, S., Alliet, M., Jáuregui-Haza, U., Albasi, C., 2008. Modelling of submerged membrane bioreactor: conceptual study about link between activated slugde biokinetics, aeration and fouling process. J. Membr. Sci. 325, 612–624.
Zhang, X., Sun, Y., Ma, F., Li, A., Yang, J., 2020. Role of soluble microbial product as an intermediate electron station linking C/N and nitrogen removal performance in sequencing batch reactor. Environ. Res. 183, 109248.
Zuthi, M.F.R., Guo, W., Ngo, H.H., Nghiem, D.L., Hai, F.I., Xia, S., Li, J., Li, J., Liu, Y., 2017. New and practical mathematical model of membrane fouling in an aerobic submerged membrane bioreactor. Bioresour. Technol. 238, 86–94.
Łagód, G., Piotrowicz, A., Cel, W., Zaburko, J., Drewnowski, J., 2019. Modeling sequencing batch reactor operational conditions depending on oxygen concentration. IOP Conference Series: Materials Science and Engineering. IOP Publishing, 012026.